Shape Preferred Orientation (OCW-UN-SPO) Launeau P. 2017

Pr. Patrick Launeau

patrick.launeau@univ-nantes.fr

The main 3D directions X, Y, Z can be retrieved at once with the following rotation:

$$\mathbf{R}_V = \begin{bmatrix} \cos\phi\cos\psi - \sin\phi\cos\theta\sin\psi & -\cos\phi\sin\psi - \sin\phi\cos\theta\cos\psi & \sin\phi\sin\theta \\ \sin\phi\cos\psi + \cos\phi\cos\theta\sin\psi & -\sin\phi\sin\psi + \cos\phi\cos\theta\cos\psi & -\cos\phi\sin\theta \\ \sin\theta\sin\psi & \sin\theta\cos\psi & \cos\theta \end{bmatrix}$$

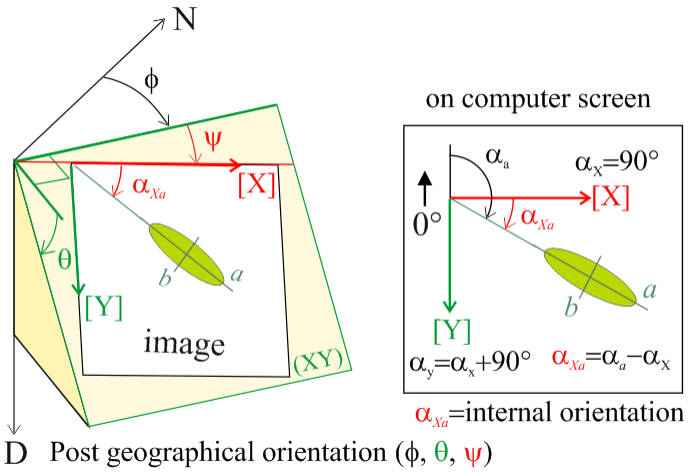

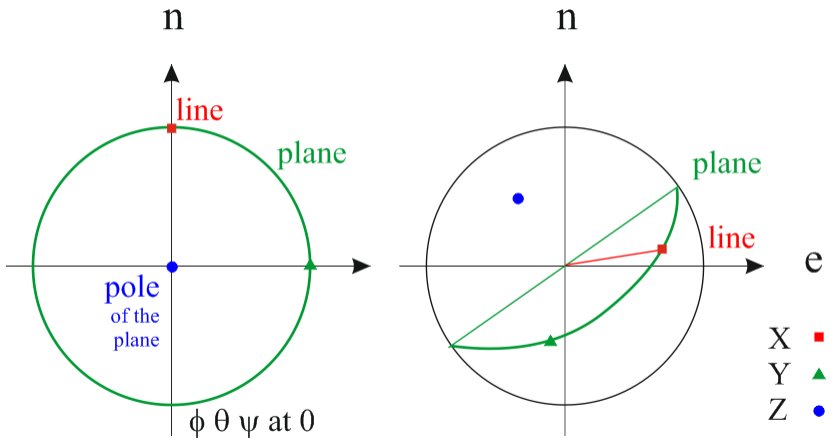

It is therefore possible to process the image in its internal coordinate system independently of its geographical orientation which can be applied afterward, on the results, by using the rotation of a volume $\mathbf{R}_V$ for which the upper face is a section (X,Y).

Launeau & Robin (2005)

Looking for 3D ellipsoid quantifications without a priori, it is recommended to cut a block sample in horizontal (NE), vertical (ED) and (ND) sections.
In such case: X || N, Y || E, Z || D.

But this is not always possible and the block sample can have its own geographical orientation which can be set by the measurement of the strike, dip and rake of its upper face (X,Y) where [X] is the rake of the first side of the block as shown in the 2nd figure.

All processing can be done in the block internal X,Y,Z coordinate system and oriented afterward in the geographic system by one rotation R_V.

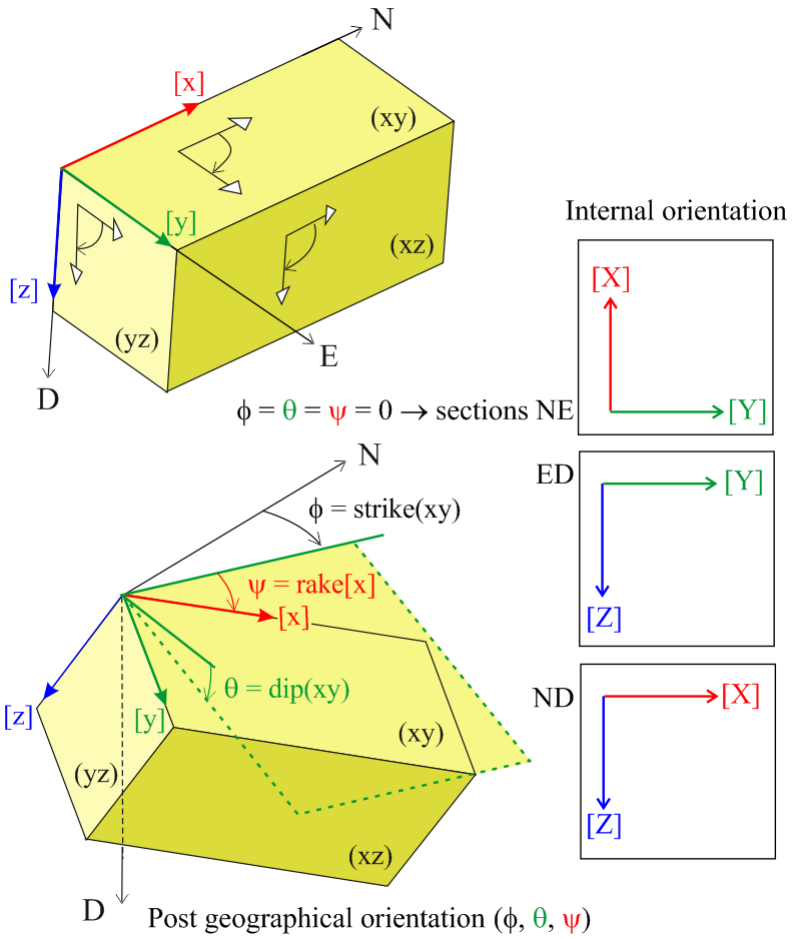

Launeau & Robin (2005)

A core drilled horizontally towards the north would have X || N, Y || E, Z || D.

This is exceptional and a core usually has its own geographical orientation which can be set by the measurement of the trend and plunge of its long axis [X] (see other convention in course 2 p. 12).
All processing can be done in the core internal X,Y,Z coordinate system and oriented afterward in the geographic system by one rotation R_V whose angle use the conversion between trend plunge in strike dip rake (see also course 2 p.12).

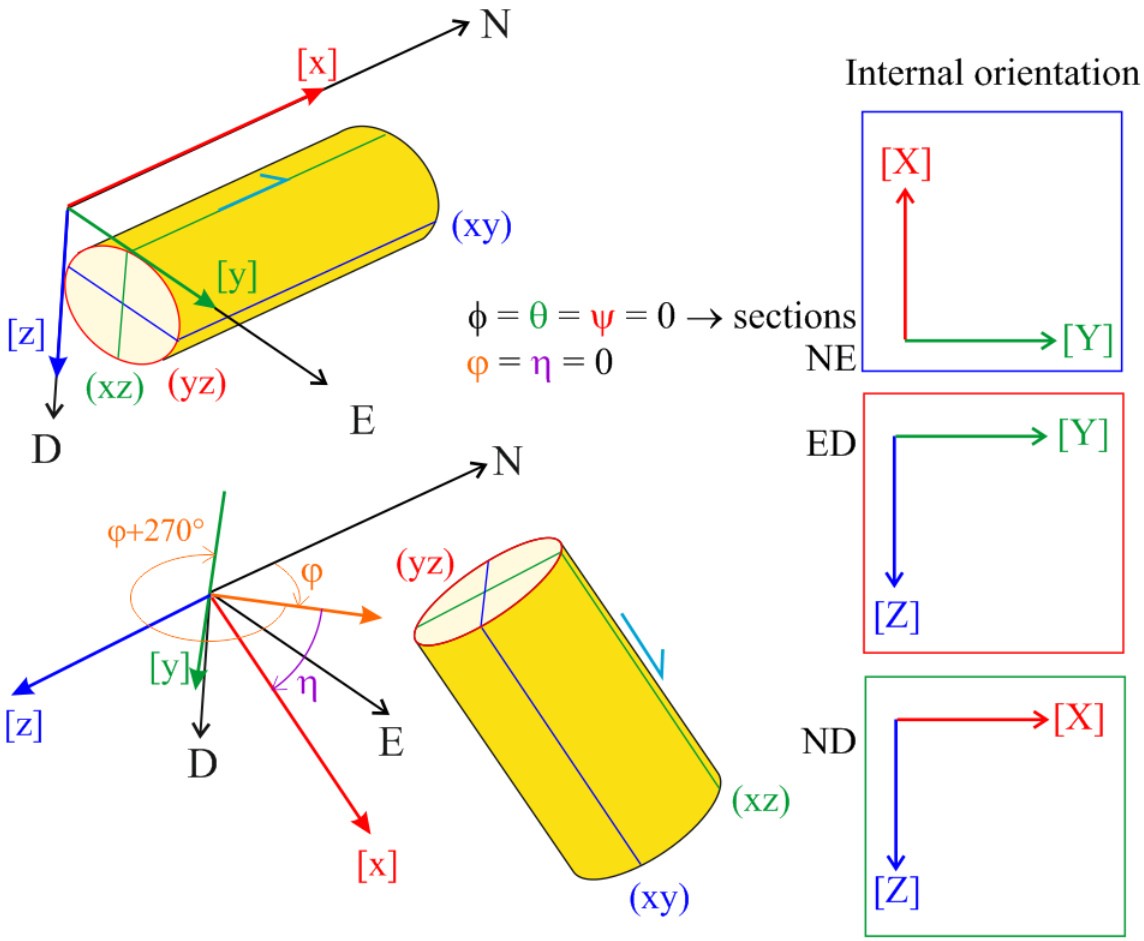

Post geographical core orientation (φ+270°, η, +90°) or (ϕ, θ, ψ)

ϕ → strike of (XY)
θ → dip of (XY)
ψ → turn back [X] in dip direction

If α_{xy} is the orientation, a_{xy} the long radius and b_{xy} the short radius of an ellipse on a (X,Y) section the drawing of any radius $l_{ellipse}$ in the direction α_{ay} required that the square of it inverse length satisfies the function →

$$\frac{1}{l(x,y)^2_{ellipse}} = \frac{\cos^2\alpha_{xy}}{a^2_{xy}} + \frac{\sin^2\alpha_{xy}}{b^2_{xy}}$$

The use of a^2 and b^2 instead of $1/a^2$ and $1/b^2$ would draw an oval →

$$l(x,y)^2_{oval} = a^2_{xy}\cdot\cos^2\alpha_{xy} + b^2_{xy}\cdot\sin^2\alpha_{xy}$$

Coordinates of an ellipse radius

$$x_{ay} = l(\alpha_{ay})\cdot\cos(\alpha_{xy}+\alpha_{ay})$$
$$y_{ay} = l(\alpha_{ay})\cdot\sin(\alpha_{xy}+\alpha_{ay})$$

Length of an ellipse radius

$$l(x,y)_{ellipse} = l(\alpha_{ay})_{ellipse} = \frac{1}{\sqrt{\frac{\cos^2\alpha_{ay}}{a^2} + \frac{\sin^2\alpha_{ay}}{b^2}}}$$

$$l(x,y)_{oval} = l(\alpha_{ay})_{oval} = \sqrt{a^2\cos^2\alpha_{ay} + b^2\sin^2\alpha_{ay}}$$

Length of an oval radius

The xy inverse shape tensor of an ellipse is therefore:

$$\mathbf{M}_{Exy} = \begin{bmatrix} \frac{1}{a^2_{xy}}\cdot\cos^2\alpha_{xy} + \frac{1}{b^2_{xy}}\cdot\sin^2\alpha_{xy} & \left(\frac{1}{a^2_{xy}} - \frac{1}{b^2_{xy}}\right)\cdot\cos\alpha_{xy}\cdot\sin\alpha_{xy} \\ \left(\frac{1}{a^2_{xy}} - \frac{1}{b^2_{xy}}\right)\cdot\cos\alpha_{xy}\cdot\sin\alpha_{xy} & \frac{1}{a^2_{xy}}\cdot\sin^2\alpha_{xy} + \frac{1}{b^2_{xy}}\cdot\cos^2\alpha_{xy} \end{bmatrix}$$

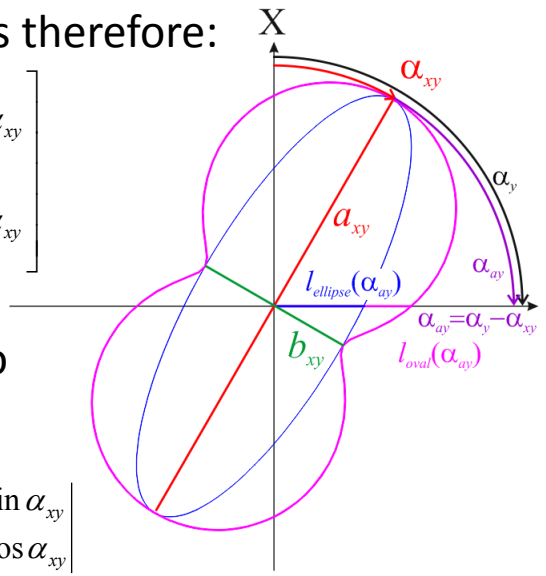

The section of a 3D ellipsoid is an ellipse with radius preserved from a section (XY) to a (YZ) or (XZ) section.

An oval cannot maintain the consistency of the radius from 2D to 3D

Which can also be written from (X,Y,Z) to $(1,2,3)$ clockwise convention as:

$$\mathbf{B}_{12} = \begin{vmatrix} b_{11} & b_{12} \\ b_{12} & b_{22} \end{vmatrix} = \begin{vmatrix} \cos\alpha_{xy} & -\sin\alpha_{xy} \\ \sin\alpha_{xy} & \cos\alpha_{xy} \end{vmatrix} \cdot \begin{vmatrix} 1/a^2_{xy} & 0 \\ 0 & 1/b^2_{xy} \end{vmatrix} \cdot \begin{vmatrix} \cos\alpha_{xy} & \sin\alpha_{xy} \\ -\sin\alpha_{xy} & \cos\alpha_{xy} \end{vmatrix}$$

Shimamoto & Ikeda's (1976), Launeau & Cruden (1998), Robin (2002), Launeau (2004), Launeau & Robin (2005).

Similarly the *xyz* inverse shape tensor of a 3D ellipsoid can be written with (1,2,3) convention:
This 3D ellipsoid can be divided in 3 perpendicular 2D sections (1,2), (1,3) and (2,3)

$$\frac{1}{l(x,y,z)^2}=\frac{x^2}{a^2}+\frac{y^2}{b^2}+\frac{z^2}{c^2}$$

$$\mathbf{B}_{123}=\begin{bmatrix} b_{11} & b_{12} & b_{13} \\ b_{12} & b_{22} & b_{23} \\ b_{13} & b_{23} & b_{33} \end{bmatrix}=\mathbf{R}_V\cdot\begin{bmatrix} 1/a^2 & 0 & 0 \\ 0 & 1/b^2 & 0 \\ 0 & 0 & 1/c^2 \end{bmatrix}\cdot\mathbf{R}_V^{-1}$$

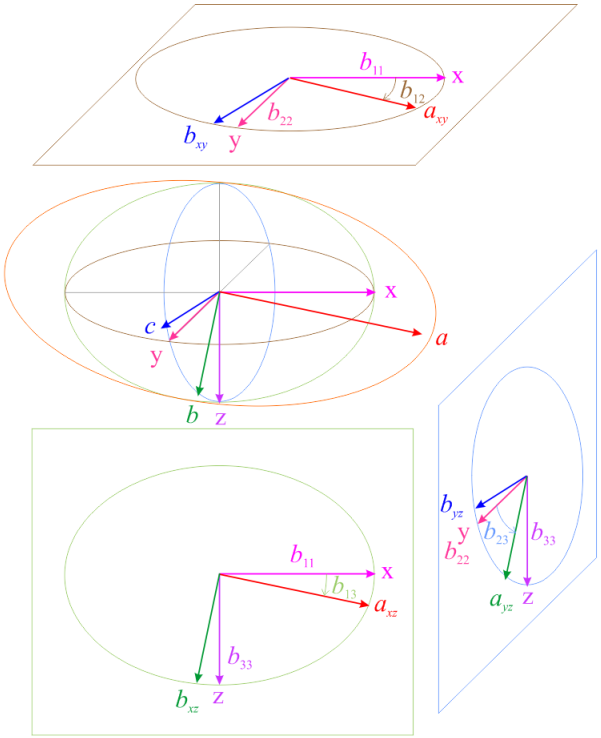

$$\mathbf{B}_{12}=\begin{vmatrix} b_{11} & b_{12} \\ b_{12} & b_{22} \end{vmatrix}=\begin{vmatrix} \cos\alpha_{12} & -\sin\alpha_{12} \\ \sin\alpha_{12} & \cos\alpha_{12} \end{vmatrix}\cdot\begin{vmatrix} 1/a_{12}^2 & 0 \\ 0 & 1/b_{12}^2 \end{vmatrix}\cdot\begin{vmatrix} \cos\alpha_{12} & \sin\alpha_{12} \\ -\sin\alpha_{12} & \cos\alpha_{12} \end{vmatrix}$$

$$\mathbf{B}_{13}=\begin{vmatrix} b_{11} & b_{13} \\ b_{13} & b_{33} \end{vmatrix}=\begin{vmatrix} \cos\alpha_{13} & -\sin\alpha_{13} \\ \sin\alpha_{13} & \cos\alpha_{13} \end{vmatrix}\cdot\begin{vmatrix} 1/a_{13}^2 & 0 \\ 0 & 1/b_{13}^2 \end{vmatrix}\cdot\begin{vmatrix} \cos\alpha_{13} & \sin\alpha_{13} \\ -\sin\alpha_{13} & \cos\alpha_{13} \end{vmatrix}$$

$$\mathbf{B}_{23}=\begin{vmatrix} b_{22} & b_{23} \\ b_{23} & b_{33} \end{vmatrix}=\begin{vmatrix} \cos\alpha_{23} & -\sin\alpha_{23} \\ \sin\alpha_{23} & \cos\alpha_{23} \end{vmatrix}\cdot\begin{vmatrix} 1/a_{23}^2 & 0 \\ 0 & 1/b_{23}^2 \end{vmatrix}\cdot\begin{vmatrix} \cos\alpha_{23} & \sin\alpha_{23} \\ -\sin\alpha_{23} & \cos\alpha_{23} \end{vmatrix}$$

SPO α, a and b parameters can be converted in 2D tensors whose components can be combined in a 3D tensor whose eigenvectors and eigenvalues give ellipsoid orientation ϕ, θ, ψ and radius a, b, c.

$$\mathbf{B}_{123}=\begin{vmatrix} \bar{b}_{11} & b_{12} & b_{13} \\ b_{12} & \bar{b}_{22} & b_{23} \\ b_{13} & b_{23} & \bar{b}_{33} \end{vmatrix}\qquad\begin{vmatrix} 1/a^2 & 0 & 0 \\ 0 & 1/b^2 & 0 \\ 0 & 0 & 1/c^2 \end{vmatrix}=\mathbf{R}_V^{-1}\cdot\mathbf{B}_{123}\cdot\mathbf{R}_V$$

The mean value of b_{11} is calculated from 2 sections (1,2) and (1,3) whereas b_{12} is given once by the section (1,2).
Such combination required a perfect determination of the length in mutually perpendicular images and a lake of scale consistency between sections may gives false results.

Shimamoto & Ikeda's (1976), Launeau & Cruden (1998), Robin (2002), Launeau & Robin (2005)

P.Y. Robin (2002) generalized the method by considering I sections $\mathbf{L}$ of the $\mathbf{B}_{123}$ ellipsoid. The I^{th} $\mathbf{B}^{I}_{23}$ ellipse is on its internal coordinate system on a plane 23 $\perp$ 1 and is taken on a section $\mathbf{L}^{I}_{23}$ of the $\mathbf{B}_{123}$ ellipsoid. In the following equation $\mathbf{X}^{I}$ allows the search of the deviation between the I^{th} measured ellipse and the effective section of $\mathbf{B}_{123}$ ellipsoid.

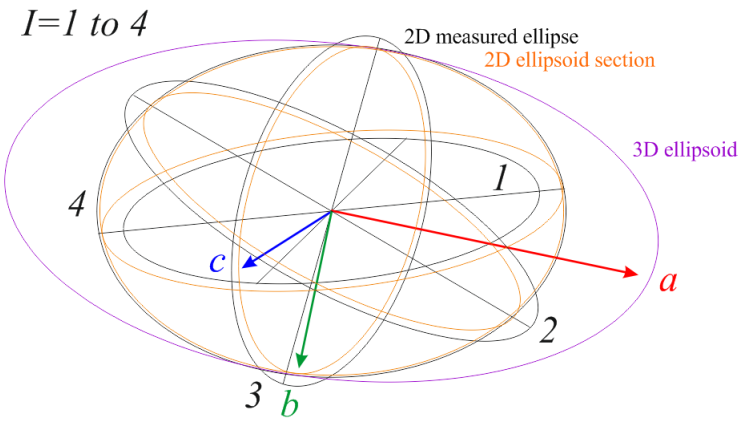

$$\mathbf{B}^{I}_{23} = \mathbf{L}^{IT}_{23} \cdot \mathbf{B}_{123} \cdot \mathbf{L}^{I}_{23} + \mathbf{X}^{I}$$

with

$$\mathbf{X}^{I} = \begin{bmatrix} \chi^{I}_{22} & \chi^{I}_{23} \\ \chi^{I}_{23} & \chi^{I}_{33} \end{bmatrix}$$

deviations to measurements

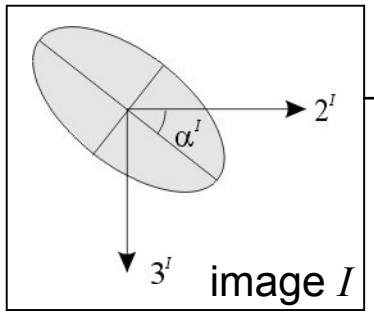

$$\mathbf{B}^{I}_{23} = \begin{bmatrix} b^{I}_{22} & b^{I}_{23} \\ b^{I}_{23} & b^{I}_{33} \end{bmatrix}$$

of the section

$$\mathbf{L}^{I}_{23} = \begin{bmatrix} l^{I}_{21} & l^{I}_{31} \\ l^{I}_{22} & l^{I}_{32} \\ l^{I}_{23} & l^{I}_{33} \end{bmatrix}$$

of ellipsoid $\mathbf{B}_{123}$

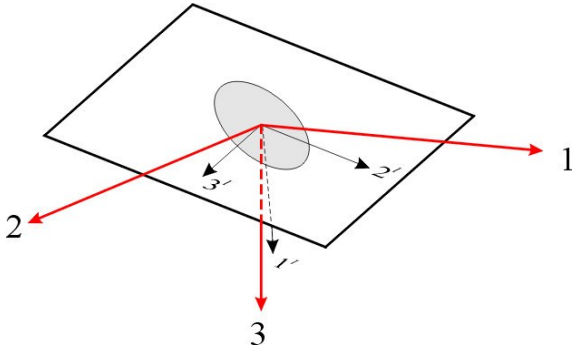

Coordinates 1^I,2^I,3^I of the I^{th} section in the ellipsoid coordinate frame1,2,3

Shape Preferred Orientation (OCW-UN-SPO) Launeau P. 2017

This method also use inverse shape tensor ellipse which can be written directly **with scale factor** of the I^{th} section SPO:

- a_I and b_I radius length;
- R_I shape ratio weighted by surface area A_I.

The method works also **without scale factor** with the calculation of a scaling factor f^I.

The calculation of $\mathbf{B}_{123}$ by Robin (2002) minimizes a scalar incompatibility index $\sqrt{\widetilde{F}}$ which is a measure of the misfit between sectional ellipses and the ellipsoid sought. It use F^B and F^I Frobenius norm (see details in the related reference) minimizing $\mathbf{X}^I$ in:

$$\mathbf{B}_{23}^I = \mathbf{L}_{23}^{IT} \cdot \mathbf{B}_{123} \cdot \mathbf{L}_{23}^I + \mathbf{X}^I$$

providing an incompatibility index for each I^{th} section:

$$\sqrt{F_{\min}^I}$$

Finally the P.Y. Robin (2002) method produces an ellipsoid $\mathbf{B}_{123}$ as 3D tensor whose eigenvectors and eigenvalues give ellipsoid orientation ϕ, θ, ψ and radius a, b, c.

Rewritten here in clockwise image coordinate system

$$\mathbf{B}_{23}^I = \begin{vmatrix} \cos\alpha_I & -\sin\alpha_I \\ \sin\alpha_I & \cos\alpha_I \end{vmatrix} \cdot \begin{vmatrix} 1/a_I^2 & 0 \\ 0 & 1/b_I^2 \end{vmatrix} \cdot \begin{vmatrix} \cos\alpha_I & \sin\alpha_I \\ -\sin\alpha_I & \cos\alpha_I \end{vmatrix}$$

$$\mathbf{B}_{23}^I = \begin{vmatrix} \cos\alpha_I & -\sin\alpha_I \\ \sin\alpha_I & \cos\alpha_I \end{vmatrix} \cdot \frac{1}{A_I} \cdot \begin{vmatrix} 1/R_I & 0 \\ 0 & R_I \end{vmatrix} \cdot \begin{vmatrix} \cos\alpha_I & \sin\alpha_I \\ -\sin\alpha_I & \cos\alpha_I \end{vmatrix}$$

$$\mathbf{B}_{23}^I = f^I \cdot \begin{vmatrix} \cos\alpha_I & -\sin\alpha_I \\ \sin\alpha_I & \cos\alpha_I \end{vmatrix} \cdot \begin{vmatrix} 1/R & 0 \\ 0 & R \end{vmatrix} \cdot \begin{vmatrix} \cos\alpha_I & \sin\alpha_I \\ -\sin\alpha_I & \cos\alpha_I \end{vmatrix}$$

$$\begin{vmatrix} 1/a^2 & 0 & 0 \\ 0 & 1/b^2 & 0 \\ 0 & 0 & 1/c^2 \end{vmatrix} = \mathbf{R}_V^{-1} \cdot \mathbf{B}_{123} \cdot \mathbf{R}_V$$

All calculations can be done either in a block sample internal coordinates system and oriented afterward at once by a rotation towards the geographic system. All calculations can also be done directly in the geographic coordinate system by substituting the relative orientation α_I by the geographic rake ψ_I of each ϕ θ section I.

In case of 3 perpendicular sections the calculation of $\mathbf{B}_{123}$ is much simpler and the incompatibility index becomes

$$\begin{bmatrix} b_{11} & b_{12} & b_{13} \\ b_{21} & b_{22} & b_{23} \\ b_{31} & b_{23} & b_{33} \end{bmatrix} = \begin{bmatrix} (b_{33}^2 + b_{22}^3)/2 & b_{23}^3 & b_{23}^2 \\ b_{23}^3 & (b_{22}^1 + b_{33}^3)/2 & b_{23}^1 \\ b_{23}^2 & b_{23}^1 & (b_{33}^1 + b_{22}^2)/2 \end{bmatrix}$$

$$\widetilde{F} = \frac{1}{6} \frac{(b_{33}^2 - b_{22}^3)^2 + (b_{22}^1 - b_{33}^3)^2 + (b_{33}^1 - b_{22}^2)^2}{(b_1)^2 + (b_2)^2 + (b_3)^2}$$

The discrepancy between an ellipsoid measured on a plane and the corresponding section of a calculated ellipsoid can be estimated with the following equation which can work with any type of ellipse and ellipsoid. This estimation ***e*** is 0% for a perfect match and increases with the discrepancy:

$$e_{ab} = \frac{2 \cdot l_{ab}}{a_c + b_c}$$

$$l_{ab} = \sqrt{\left((a_m - b_m)\cdot\left|\cos(\varphi_m - \varphi_c)\right| - (a_c - b_c)\right)^2 + \left((a_m - b_m)\cdot\left|\sin(\varphi_m - \varphi_c)\right|\right)^2}$$

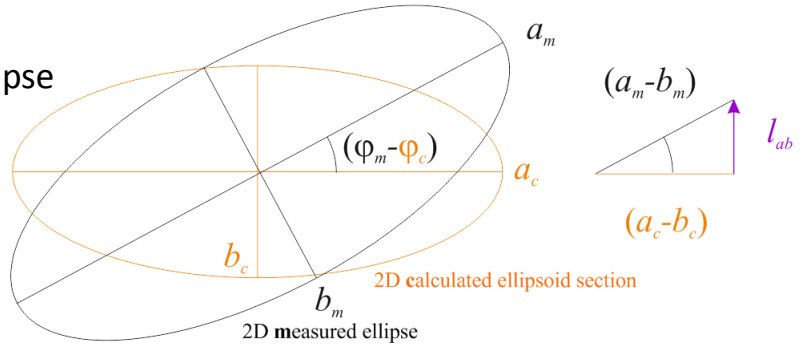

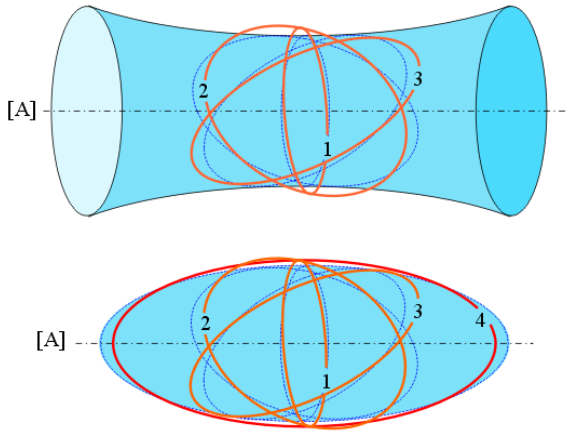

The P.Y. Robin (2002) method working with any set of a minimum of 3 sections some cases may not provide the solution for a closed ellipsoid. It may give an hyperboloid with a direction of "opening" [A], 1st figure, which can be explored on a block sample or in the field searching for a section allowing to close the ellipsoid as shown in the 2nd figure.

When 2D SPO of passive deformation are ellipses giving the strain in 2D their combination in 3D gives an ellipsoid which is the strain in 3D while the deformation are homogenous.

The SPO of rigid body rotation in active deformation along a simple shear magma flow requires some complementary warning.

Shape Preferred Orientation (OCW-UN-SPO) Launeau P. 2017

Let build a population with random orientation and typical distribution of body shape ratio ranging from 1.15 to 3.4 with a mean shape ratio 2 and simulate a 3D shear flow (see details in course 3 p.18).
The cut of all 3D ellipsoids in 2D ellipses in (XZ), (XY) and (YZ) sections will simulate their 2D image analysis and combination in 3D. A random scale factor simulating a section of ellipsoid at any distance from their gravity center makes the simulation more realistic. It is applied to 800 ellipsoids with a random initial orientation undergoing a rigid body free rotation in a magma up to a shear rate $\gamma = 30$. This is expected in a stack of 1m of magma flowing over a distance of 30m.
3D results are calculated on the 3D ellipsoids whereas 2D results are cut in 3 perpendicular sections prior their recombination in 3D ellipsoids.
$Rf^{0.5}(a/c)$ are cosine directions and $R(a/c)$ are ellipses observed on (XZ) sections.
All ellipsoid sections R results present a shift with $Rf^{0.5}$ results because of cutting effect (see also course 3 p.14).
Only ellipse inverse tensors perfectly match the ellipsoid sections:
2D ellipse $R_n(a/c)$ perfectly match 3D ellipsoid $R_n(a/c)$ and 2D ellipse $R(a/c)$ perfectly match 3D ellipsoid $R(a/c)$.
2D inertia tensor combinations in 3D give false intensities because of the lake of size consistency between perpendicular sections (see p.4).

Launeau (2004)

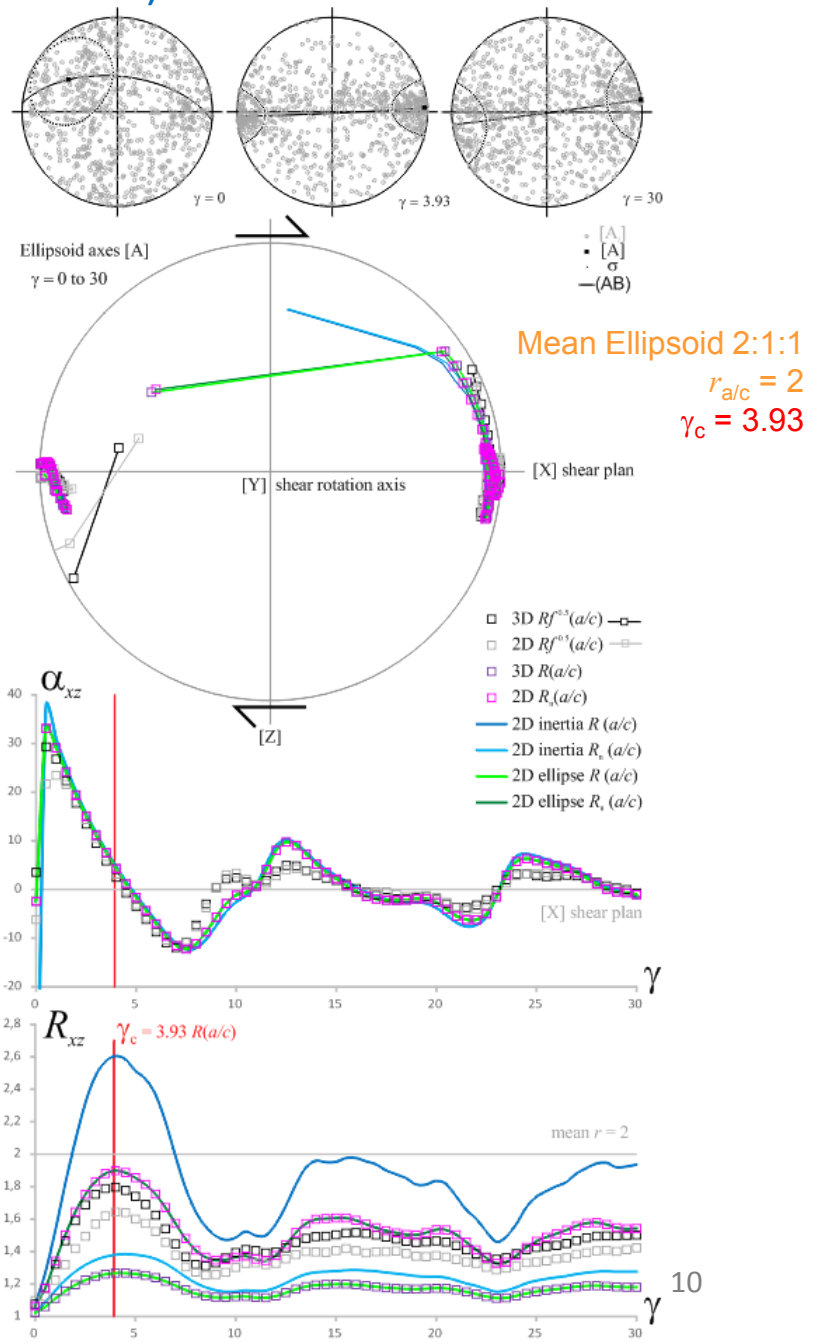

Shape Preferred Orientation (OCW-UN-SPO) Launeau P. 2017

The measurement mask, set to a quarter of the image, overlapping 50% on each other, gives 9 sub SPO per image allowing quantification of their invariance by translation. Thus, 3 mutually perpendicular images containing 9 sub SPO ellipses, can be combined one by one from each section in 9^3 or 729 sub 3D ellipsoids.

Eigenvectors and eigenvalues of the whole mean inverse tensor ellipsoid give the orientation and intensity of the main SPO ellipsoid A, B and C.

The same calculation is applied to each of the 729 sub SPO from which $\overline{X}$ mean value and σ standard deviation can be calculated for each type of data, normalized length, orientation (angular scattering cone), anisotropy parameter or compatibility index.
(See also course 4 p. 39)

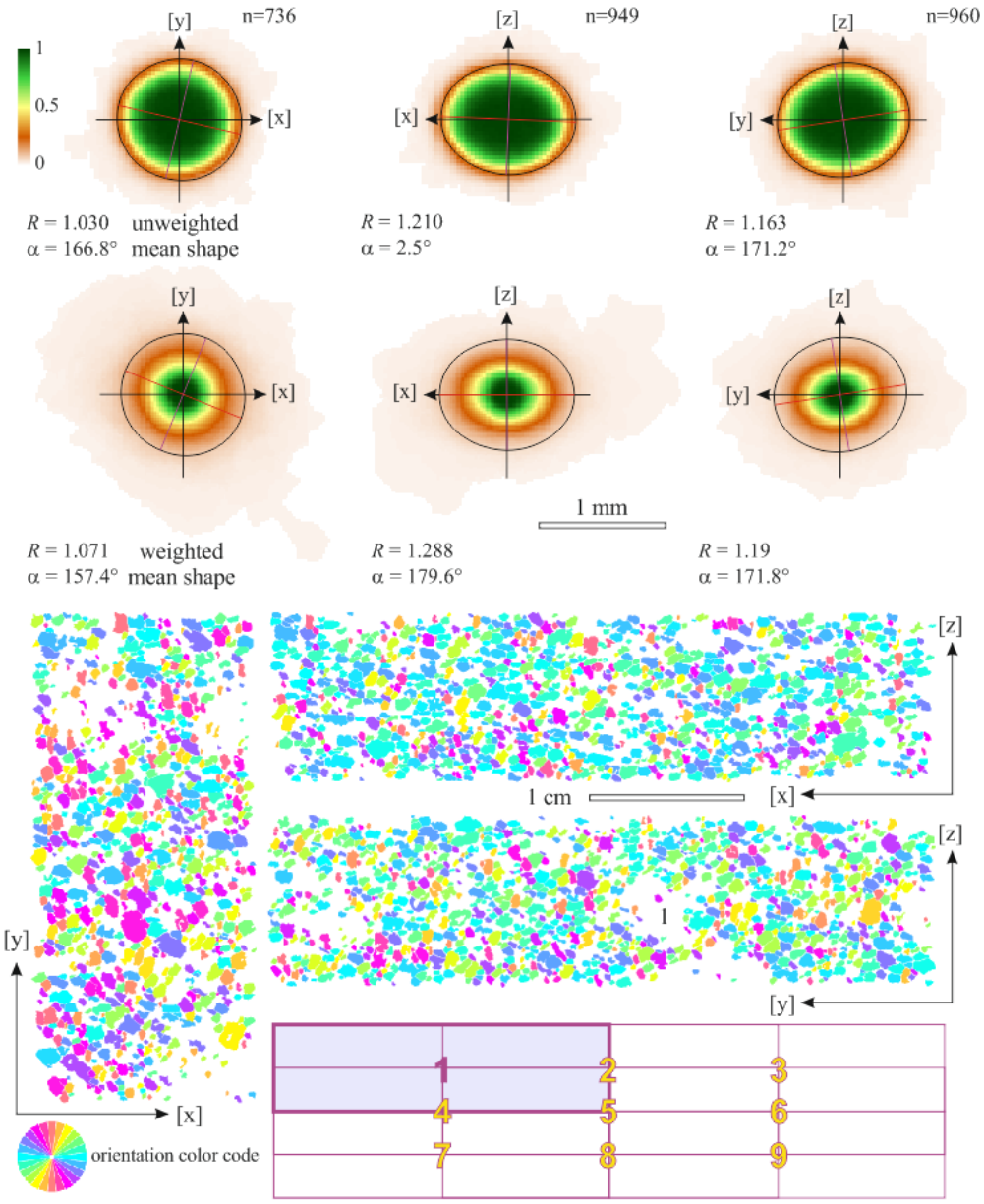

Launeau & Robin (2005)

Shape Preferred Orientation (OCW-UN-SPO) Launeau P. 2017

All ellipsoid results are combinations of inverse tensor ellipses, as it can be attested by the μ eigenvalues.
The mean tensor ellipsoids present values close to each other but the main directions are less scattered ellipsoid are build with mean weighted 2D inertia tensors (left figure), than for ellipsoid build with mean unweighted 2D inertia tensors (right figure). Small crystals may be insignificant fragments causing the scattering.

All images analyses were applied on the internal coordinates system of the block sample and the final ellipsoid are reoriented afterwards with the rotation ϕ, θ, ψ : 137°, 10°, 170°.
But this also works : 317°, -10°, -10°.

Launeau & Robin (2005)

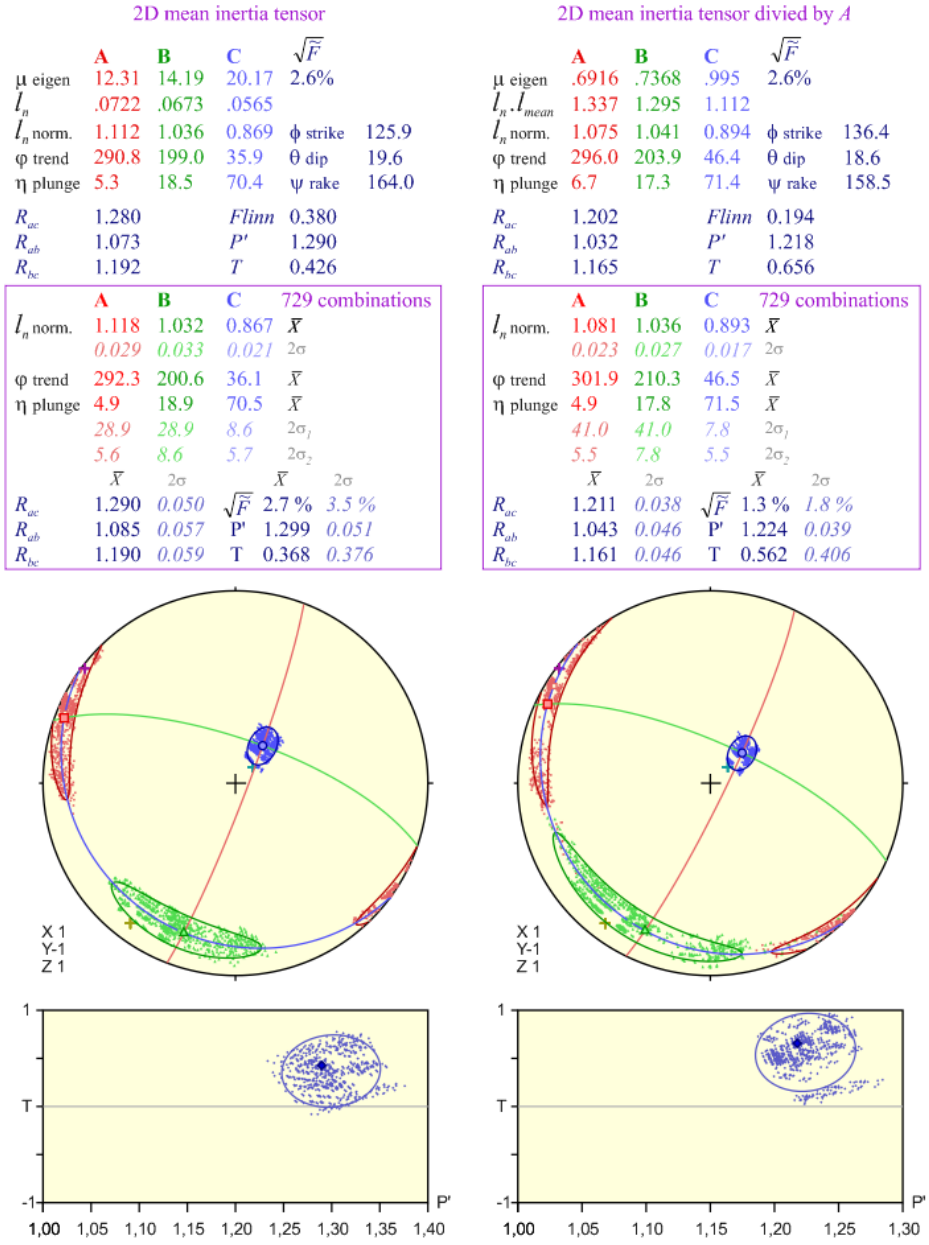

All ellipsoids are combinations of inverse tensor ellipses but they can be done with the ellipsoid calculation 1) without scale factor, including a scale factor adjustment of the sections, 2) with scale factor given by ellipse sizes measured in 2D and 3) with the direct combination of inverse tensor ellipse component. As shown on the figure below, the ellipsoid calculation with scale factor is equal to the simple 2D tensor component averaging in a 3D tensor which however works only on strict perpendicular sections.

Ellipsoid without scale factor
See p. 8

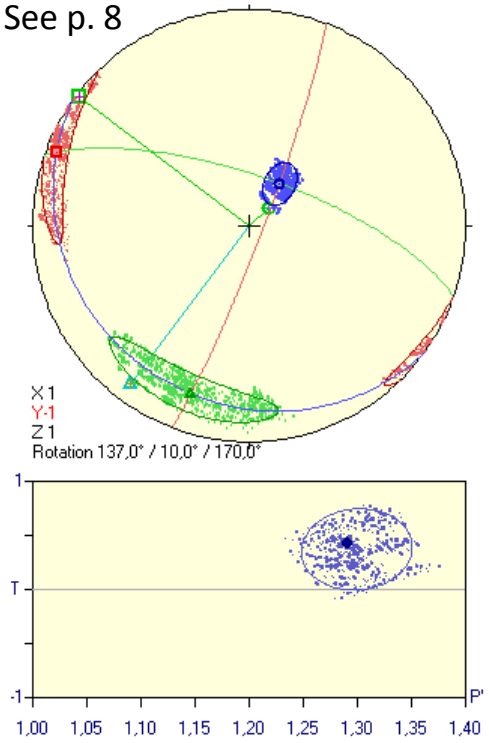

Ellipsoid with scale factor
See p.8

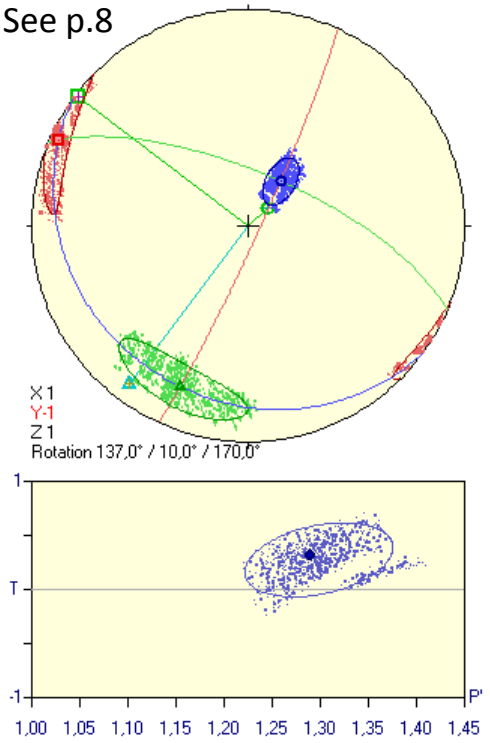

Ellipsoid mean of tensor components
See p.6

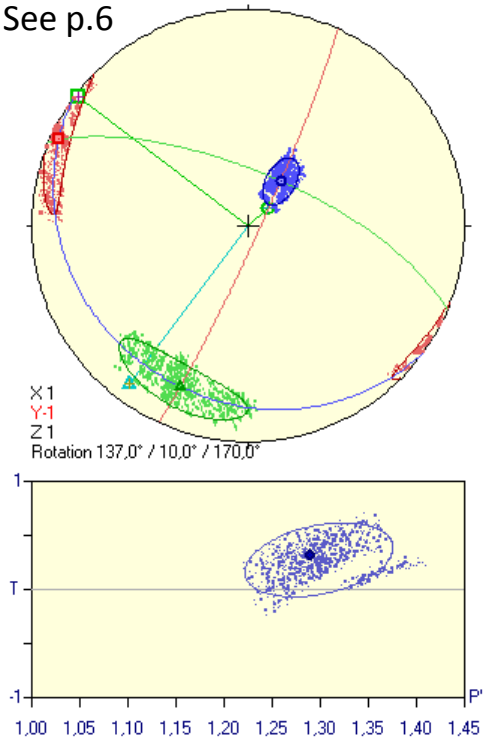

Shape Preferred Orientation (OCW-UN-SPO) Launeau P. 2017

The order of crystallization also play a role in the formation of mineral SPO like in the other example of gabbronorite from the Bushveld presented in course 4 p. 40.
The OPX crystallizing among the first minerals displays SPO consistent with the magmatic flow direction whereas the plagioclase presenting late overgrowth presents lineation scattering.

The intercepts SPO being sensitive only to crystal boundaries the method detect earliest crystals orientation distributions before their aggregation by overgrowth.
This legitimate the use of intercepts method in magma flow studies.

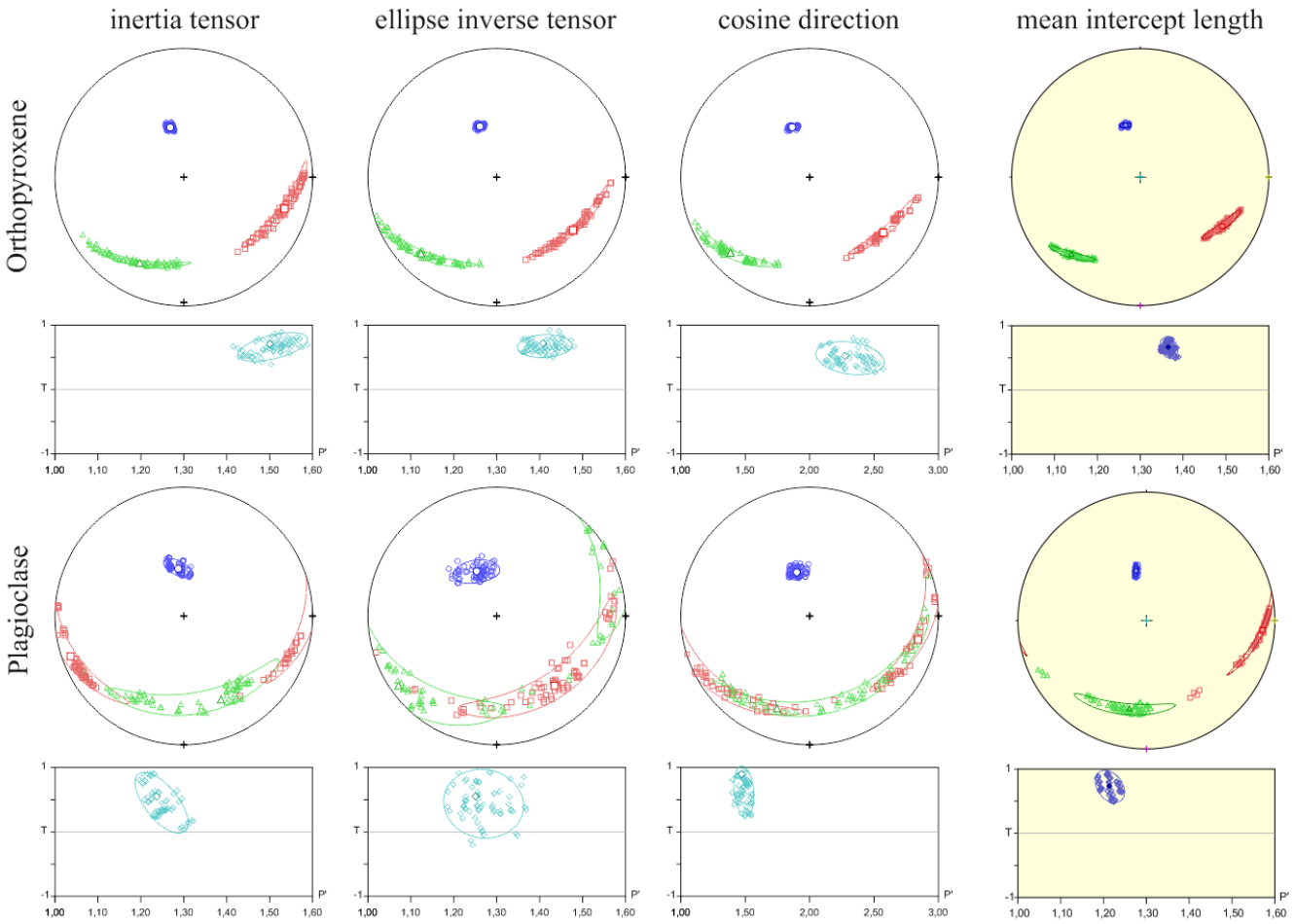

This example of SPO obtained with intercepts of one phase made of ilmenite and magnetite (Tellnes norite from Norway) organized in aggregates of crystals show once again a good correspondence between AMS and SPO.

The intercepts method does not considering image borders it is not sensitive to shape of the area of analysis. For instance a disk presenting a smaller surface area gives more scattered data than a rectangle presenting a larger surface area of analysis.

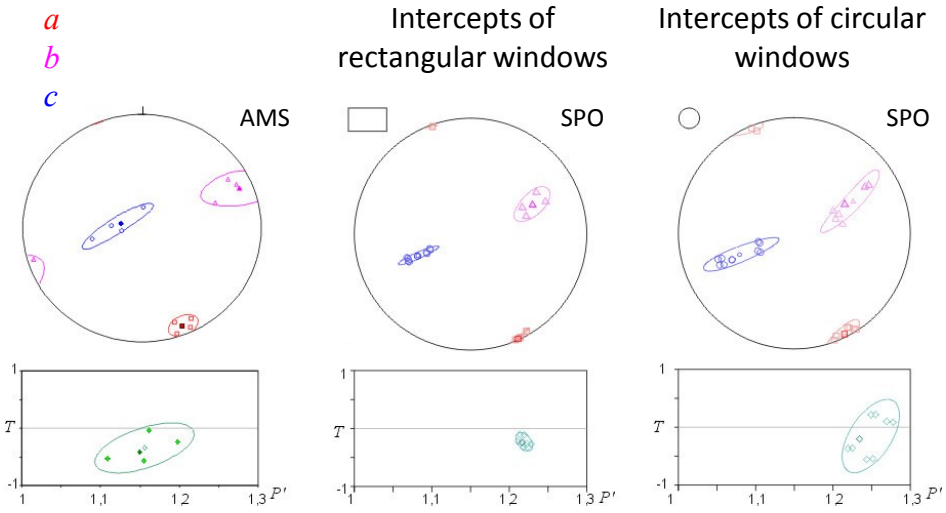

Launeau & Robin (2005)

Grey level threshold on dark minerals

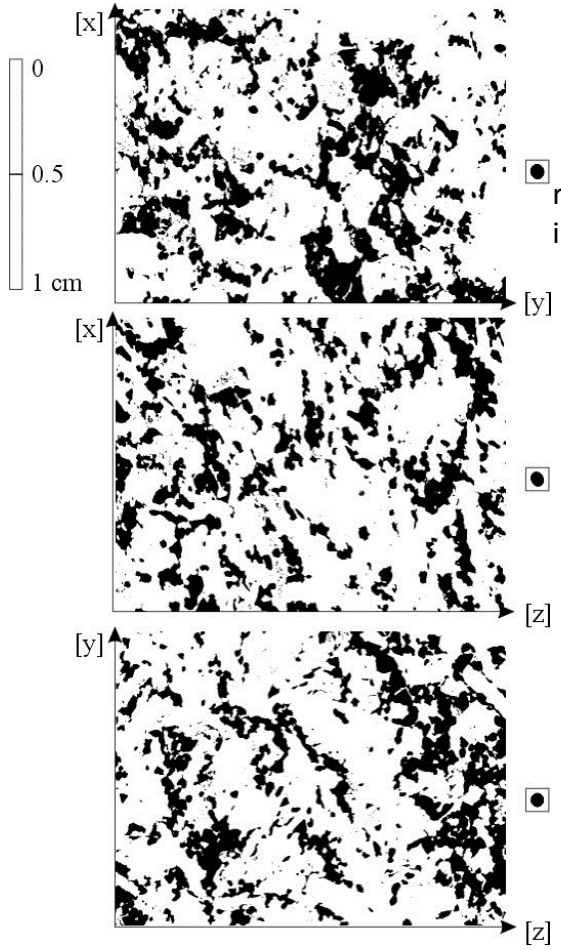

H. Diot *et al.* 2002

This application to the analysis of analog modeling displays a good correspondence between volumetric AMS (anisotropy of magnetic susceptibility) measurements and 3D SPO ellipsoid given by the combination of 2D inverse tensor ellipses.

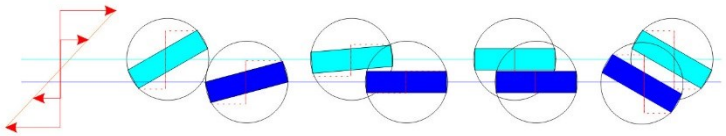

The greater angle of obliquity between SPO and AMS with the flow shear plan probably comes from an effect of grain interactions as shown in the figure above.

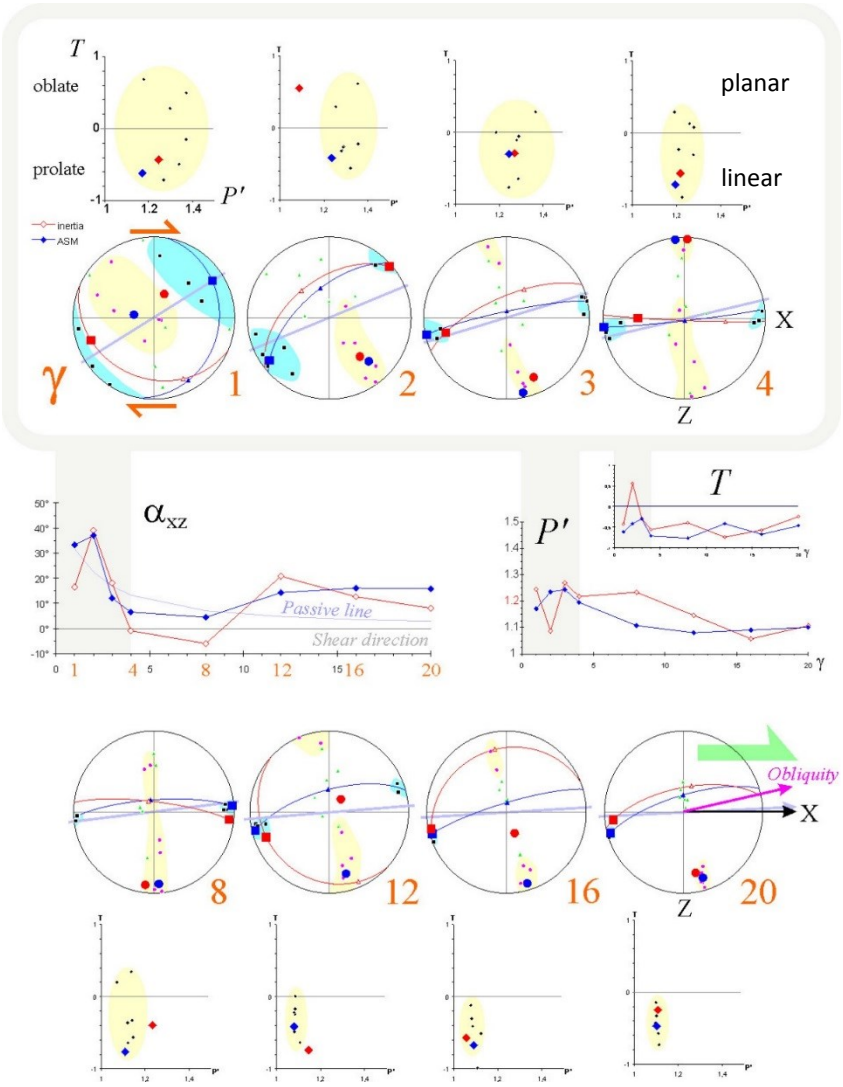

Arbaret *et al.* (2000, 2013)

Shape Preferred Orientation (OCW-UN-SPO) Launeau P. 2017

The method is also applicable to sedimentary rock like in this case of undeformed sandstone from the Paraná Basin (Brazil). The calculated SPO can record the cross-bedding of sand waves produced by down current migration towards the basin paleo slope.

All images are sections of a core orientation φ, η : 345°, 0° with an arrows [x] drawn on its elongation axis giving the rotation ϕ, θ, ψ : 0°, 0°, 15°.

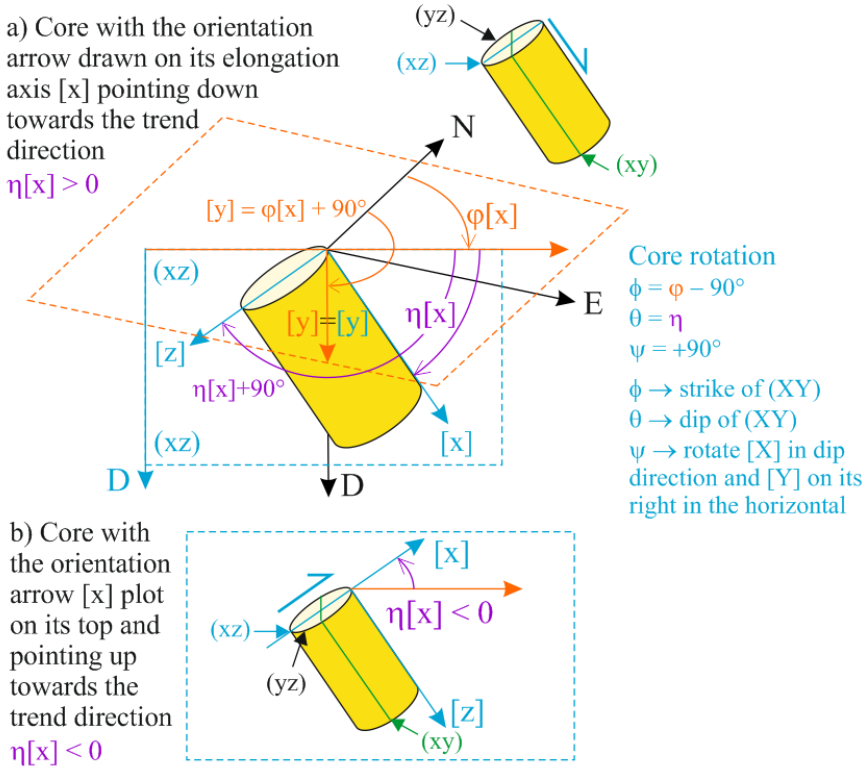

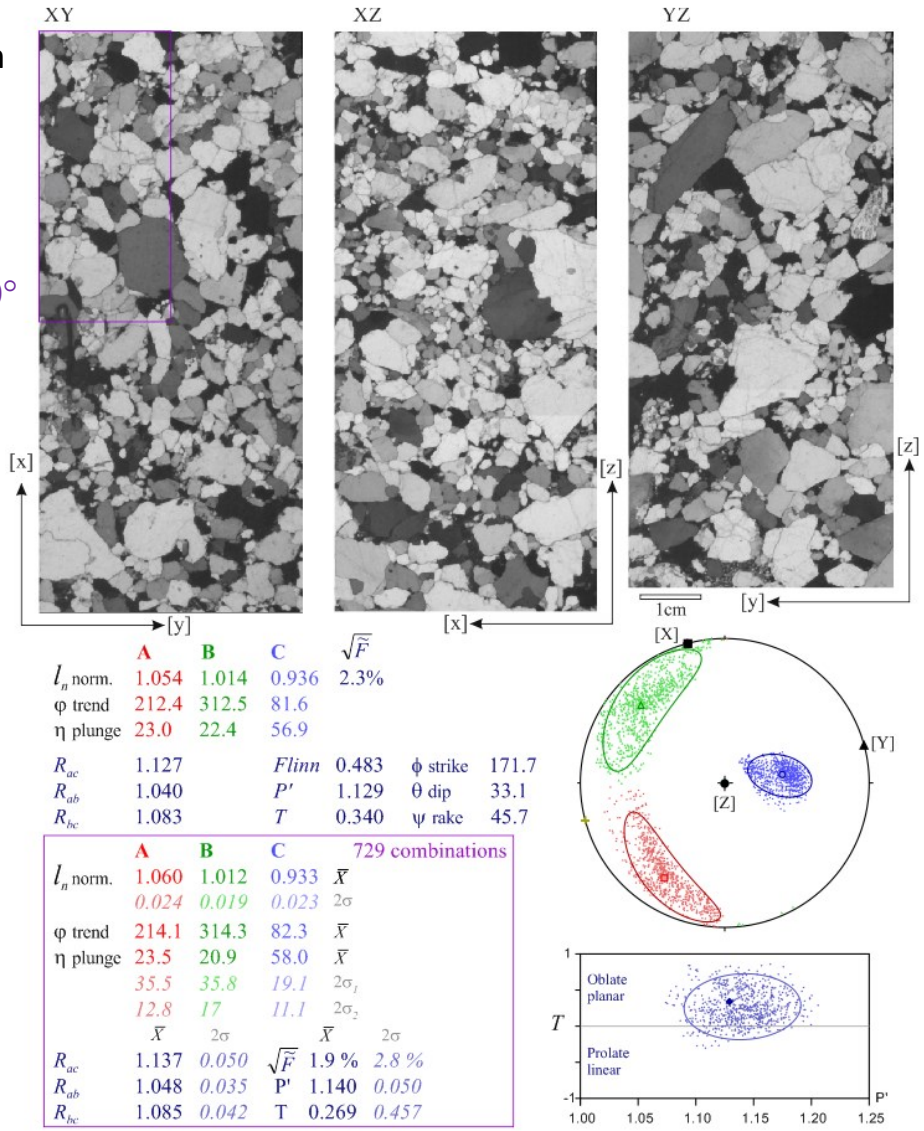

Archanjo *et al.* (2006), Launeau *et al.* (2010)

Shape Preferred Orientation (OCW-UN-SPO) Launeau P. 2017

This example is a maximum polarized light, using Fueten and Goodchild (2001) methodology. The specimen comes from about 3 cm from the margin of a Mesozoic diabase dike (Rio Ceará-Mirim swarm, NE Brazil) .

The core orientation is $\varphi, \eta : 318°, 77°$ with an arrows [x] drawn on its elongation axis gives the core rotation : $\phi, \theta, \psi : 228°, 77°, 90°$.
See core type a p. 16.

The 3 thin sections images, of each 4 core sections, were processed in the (X,Y,Z) internal coordinate system with an inclination angle of 8° (YZ up side down) and reoriented in the (N,E,D) geographic system afterward.

The 4096 ellipsoids display a prolate SPO consistent with the scattering of the [B] and [C] axes around the axis [A].

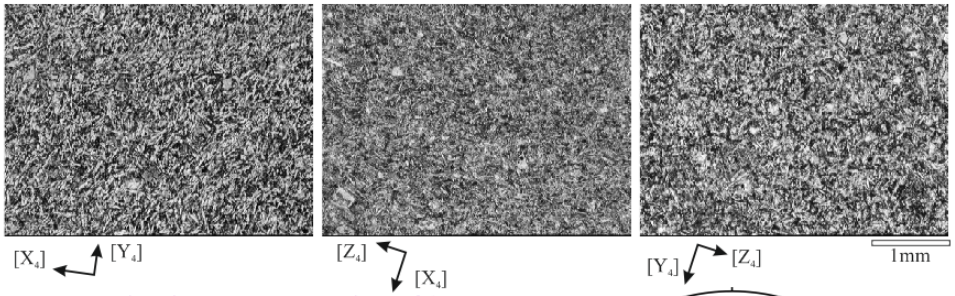

2D mean inertia tensor per 3 sections of 4 cores

	A	B	C	$\sqrt{\tilde{F}}$	
μ eigen	7.82	10.36	10.75	2.1%	
l_n	.1152	.1001	.0982		
l_n norm.	1.105	0.960	0.942	ϕ strike	230.3
φ trend	240.2	338.8	140.3	θ dip	43.8
η plunge	9.4	42.3	46.2	ψ rake	13.6
R_{ac}	1.173		*Flinn*	7.947	
R_{ab}	1.151		*P'*	1.190	
R_{bc}	1.019		*T*	-0.764	

	A	B	C	4096 combinations
l_n norm.	1.106	0.962	0.941	$\bar{X}$
	0.010	*0.010*	*0.009*	2σ
φ trend	240.2	339.1	140.6	$\bar{X}$
η plunge	9.3	43.4	45.1	$\bar{X}$
	4.5	*33.6*	*33.6*	$2\sigma_1$
	3.2	*4.3*	*3.5*	$2\sigma_2$

	$\bar{X}$	2σ		$\bar{X}$	2σ
R_{ac}	1.176	*0.018*	$\sqrt{\tilde{F}}$	4.6 %	*1.8 %*
R_{ab}	1.150	*0.019*	P'	1.192	*0.018*
R_{bc}	1.023	*0.019*	T	-0.727	*0.217*

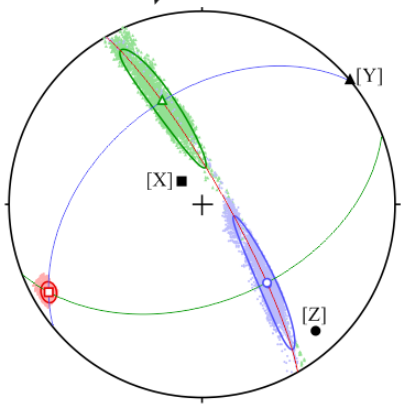

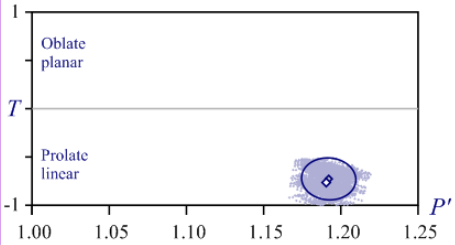

Archanjo *et al.* (2002), Launeau *et al.* (2010)